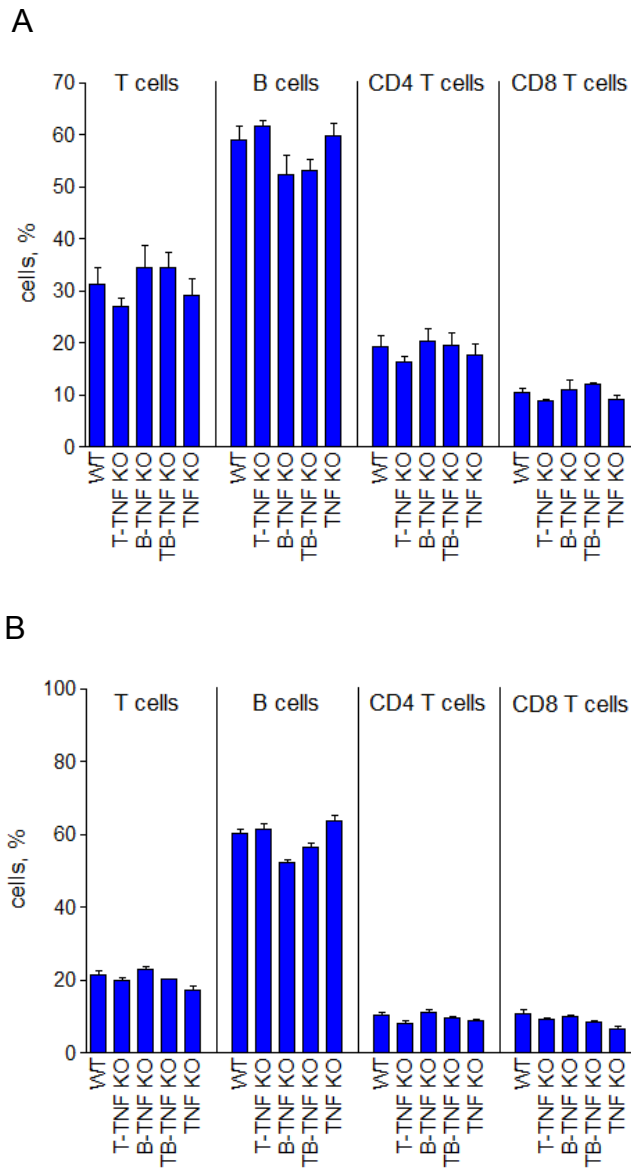
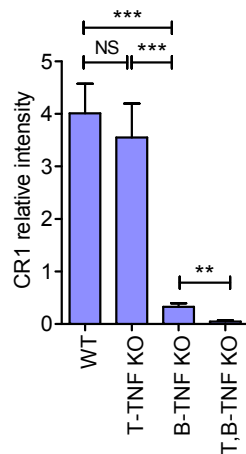
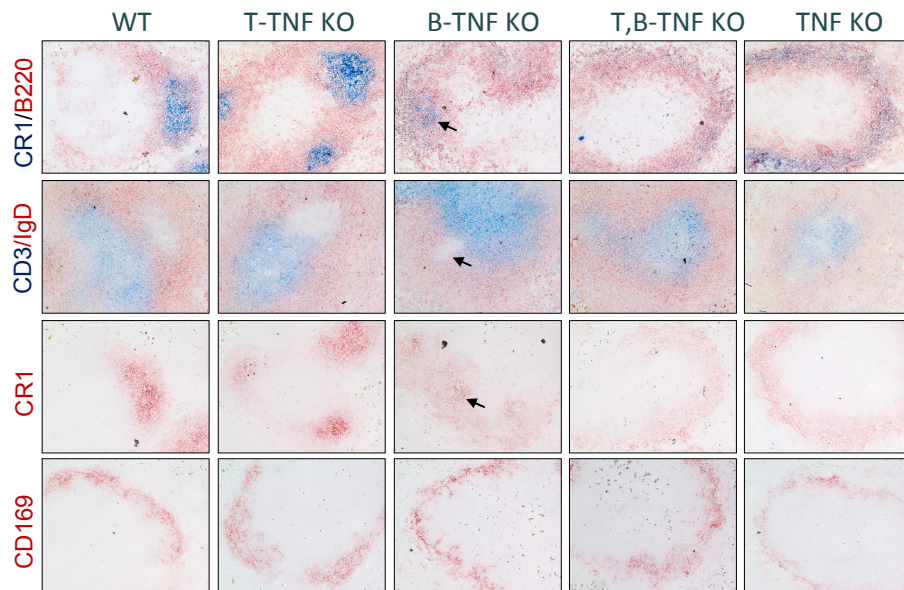


**Table S1. Sequences of oligonucleotide primers used for real-time PCR**

<b>Gene name</b>	<b>Primer name</b>	<b>Sequence</b>
CCL22	CCL22-fw CCL22-rv	TGGAGTAGCTTCTTCACCCA TCTGGACCTCAAATCCTGC
CXCL13	CXCL13-fw CXCL13-rv	TTGTGTAATGGGCTTCCAGA AGGTTGAACTCCACCTCCAG
Serpina1a	Serpina1a-fw Serpina1a-rv	AACATCCTCAGCCAGAAAGC AGCTCTGGGACAGCAAGC
St6galnac2	St6galnac2-fw St6galnac2-rv	GTGCTCTTACCCACTGAGCC ACCAGCCAAGTTCAGAAGCA
MadCAM1	MadCAMF MadCAMR	CTGAGCCCTACATCCTGACCT GCTTCACAGAGTAGCTCCCAG
TNF	TNF-fw TNF-rv	CAGCCTCTTCTCATTCTGC GGTCTGGGCCATAGAACTGA
HPRT	HPRT-fw HPRT-rv	CTCCTCAGACCGCTTTTTG ACCTGGTTCATCATCGCTAA
GAPDH	GAPDH-fw GAPDH-rv	TTGATGGCAACAATCTCCAC CGTCCCGTAGACAAAATGGT



**Figure S1. Similar numbers of T and B cells in spleen from T- and B- cell specific TNF deficient mice.** Spleens were isolated from either SRBC-immunized (**A**) or naive (**B**) mice, single cell suspensions were prepared using cell strainer, stained with anti-CD19, anti-CD4, anti-CD8 antibodies and analyzed by flow cytometry.



**Figure S2. Generation of primary B cell follicles and FDC in naïve spleen is primarily controlled by TNF produced by B cells with distinct contribution from TNF produced by T cells.** Frozen spleen sections from naïve conditional TNF deficient mice were stained with indicated antibodies. B-TNF KO mice lack polarized B cell follicles, and organized FDC networks. Note that some FDC and IgD negative areas are present in the spleens of B-TNF KO mice (shown by arrows), while no FDC and no polarized B cell follicles are observed in spleen of T,B-TNF KO mice. Original magnification is x200. Representative images from one of two independent experiments (n=5 mice per group) are shown. Bottom panel shows quantification of CR1 positive areas. Data represent means  $\pm$  s.e.m.  $**P < 0.01$ ,  $***P < 0.001$ .

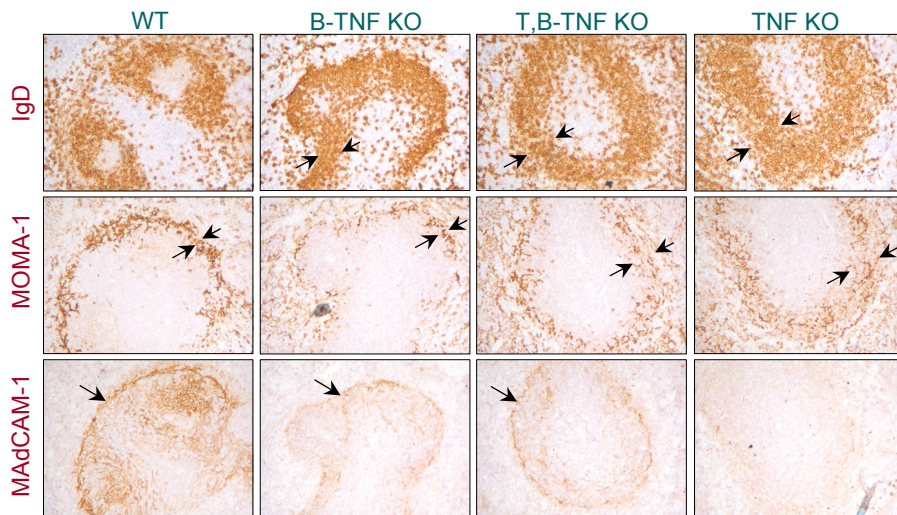


**Figure S3. Marginal zone organization in naïve spleen is controlled by TNF from B cells with additional contribution of TNF signals from T and non- T,B- cells.** Frozen spleen sections from naïve conditional TNF deficient mice were stained with anti-IgD, anti-MOMA-1, and anti-MAdCAM-1 antibodies. Note the extension of marginal zone size, disorganized layer of marginal zone macrophages and marginal sinus in B-TNF, T,B-TNF KO, and TNF KO mice compared to WT mice (shown by arrows). Original magnification is x200. Representative images from one of three independent experiments (n=5 mice per group) are shown.

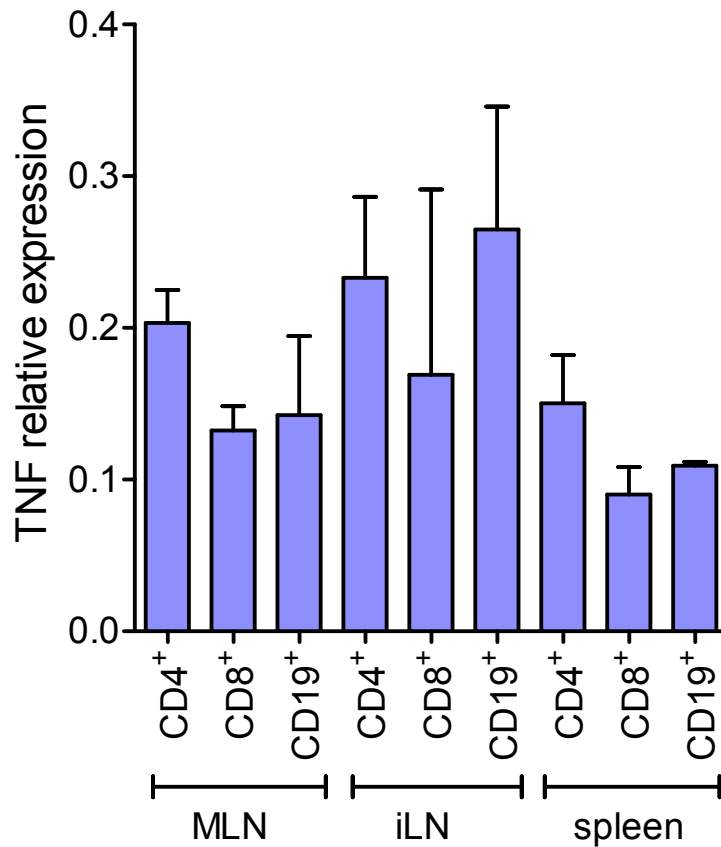


**Figure S4. TNF expression in T and B cells from spleen and LN in C57Bl/6 mice.** Similar TNF expression levels in purified T and B cells from spleen compared to mesenteric LN (MLN) and inguinal LN (iLN). Splens and LN were pooled from 3 animals, cells were purified from WT mice using positive selection magnetic bead kit from Stem Cell Technologies, according to the manufacturer's protocol, and TNF expression in CD4<sup>+</sup>, CD8<sup>+</sup>, and CD19<sup>+</sup> cells measured by real-time PCR with SYBR Green. 2 independently sorted samples were analyzed. Data represent mean values. The data were normalized to HPRT expression. One of two independent experiments with similar results is shown.

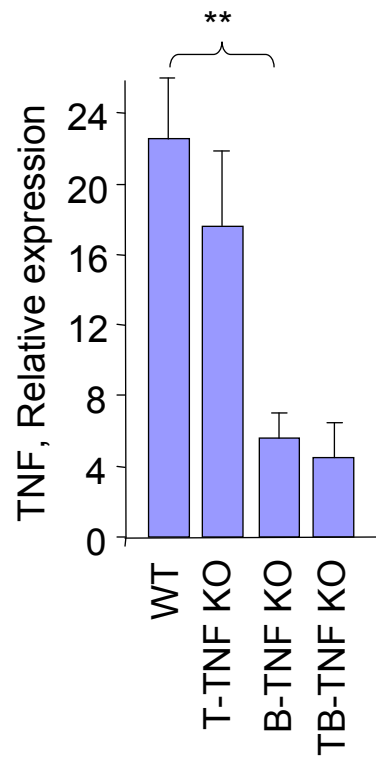


**Figure S5. TNF expression in spleen in various cell-specific TNF deficient mice.** RNA was isolated from total spleen, and TNF expression measured by real-time PCR (represents one of two independent experiments, three mice per group). The data were normalized to GAPDH expression. **\*\* $P < 0.01$ .**

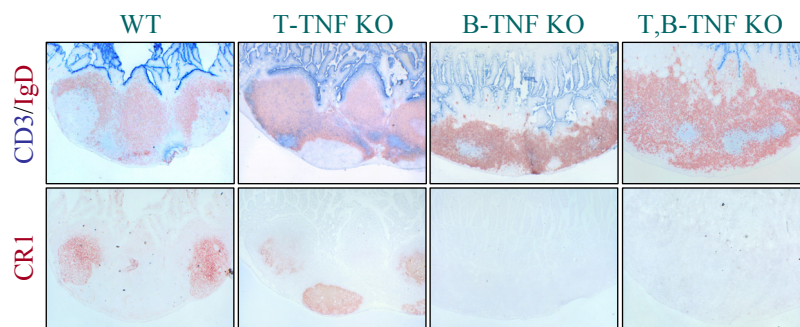


**Figure S6. TNF produced by B cells is critical for organization of PP.** Mice were immunized i.p. with 108 SRBC and PP sections analyzed on day 8. Frozen sections of PP were stained with antibodies: anti-IgD (red)/anti-CD3 (blue) and anti-CR1 (red). B-TNF KO mice lack FDC and B cell follicles while T-TNF KO mice show normal PP structure. Original magnification is x100. Representative images from one of two independent experiments (n=3 mice per group) are shown.

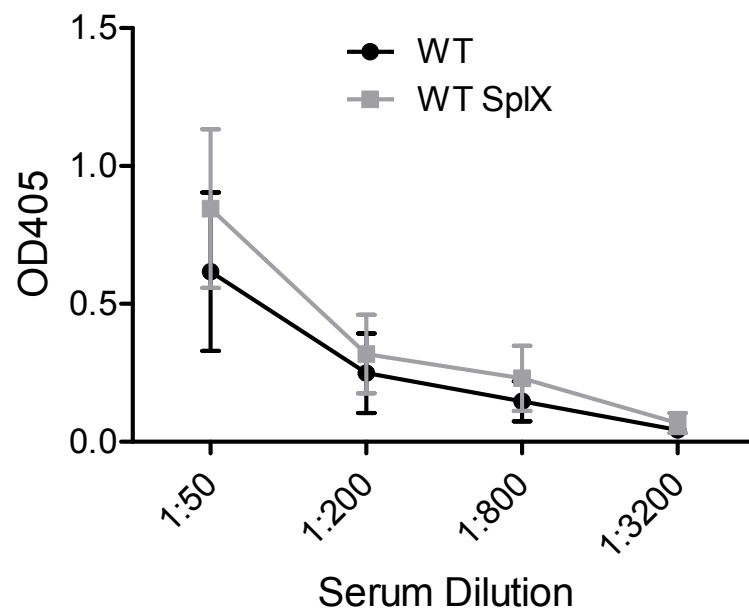


**Figure S7. Splenectomized mice are able to generate IgG response after i.p. immunization.** Splenectomized mice and control WT mice were immunized i.p. with 108 SRBC and specific IgG response measured at day 21 by ELISA. n=5 mice per group.



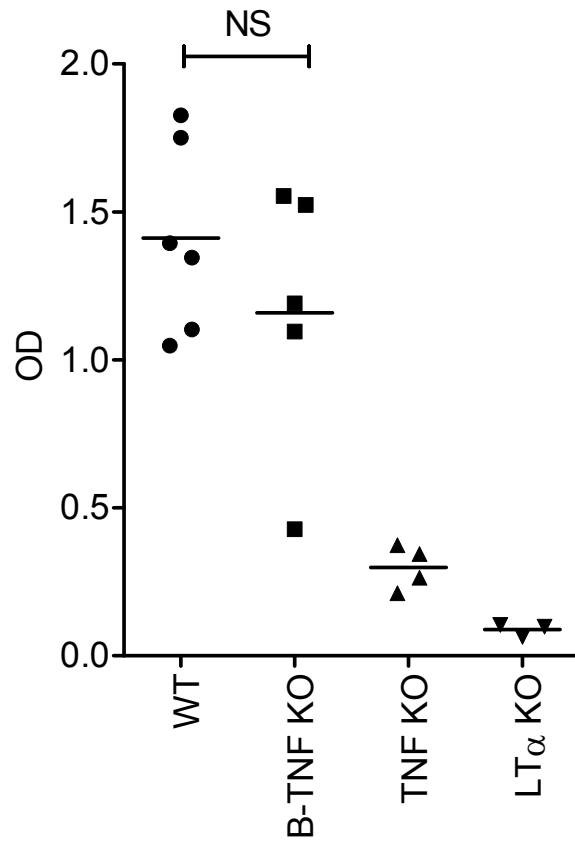


**Figure S8. Generation of memory response to SRBC is not impaired in B-TNF KO mice.** Mice were re-challenged two months after primary immunization

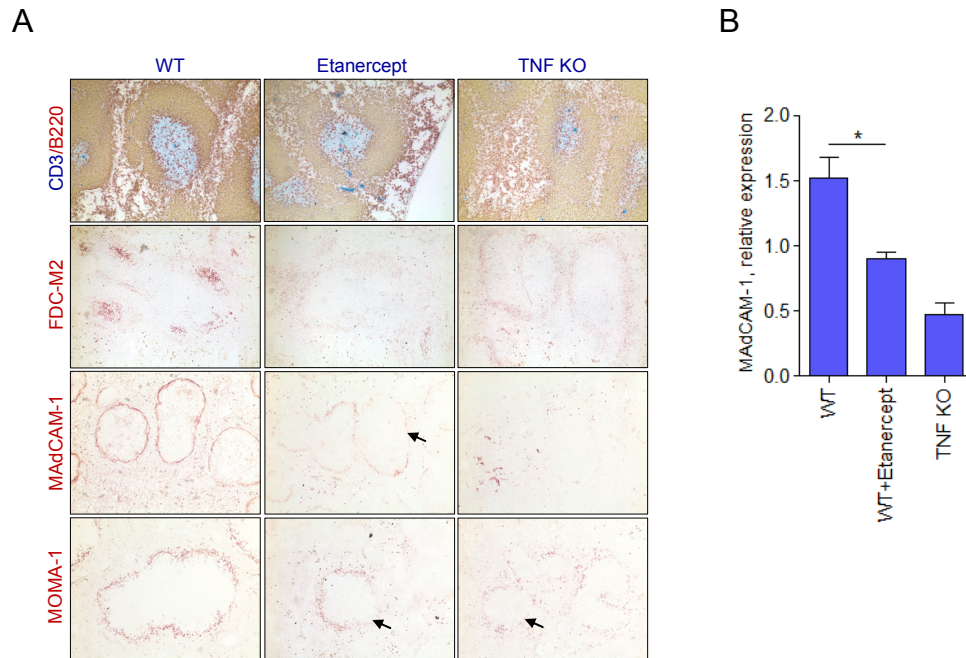


**Figure S9. Administration of TNF blocker disrupts lymphoid microarchitecture.** WT mice were injected i.p with Etanercept (p75TNFR-Ig, 30mg/kg) at day 0, 3 and 6, and spleen was analyzed by immunohistochemistry at day 7. Representative images from one of two independent experiments (n=5 mice per group) with similar results are shown. Original magnification is x200. Note that B cell follicles were disorganized after treatment and FDC were severely reduced. Interestingly, the staining for marginal zone specific markers MAdCAM-1 and MOMA-1 was also reduced after Etanercept administration, suggesting that the integrity of the marginal zone can be affected after anti-TNF therapy. **B.** Expression of MAdCAM-1 in spleen of indicated mice. n=5 mice per group. Data represent means  $\pm$  s.d. \* $P < 0.05$ .

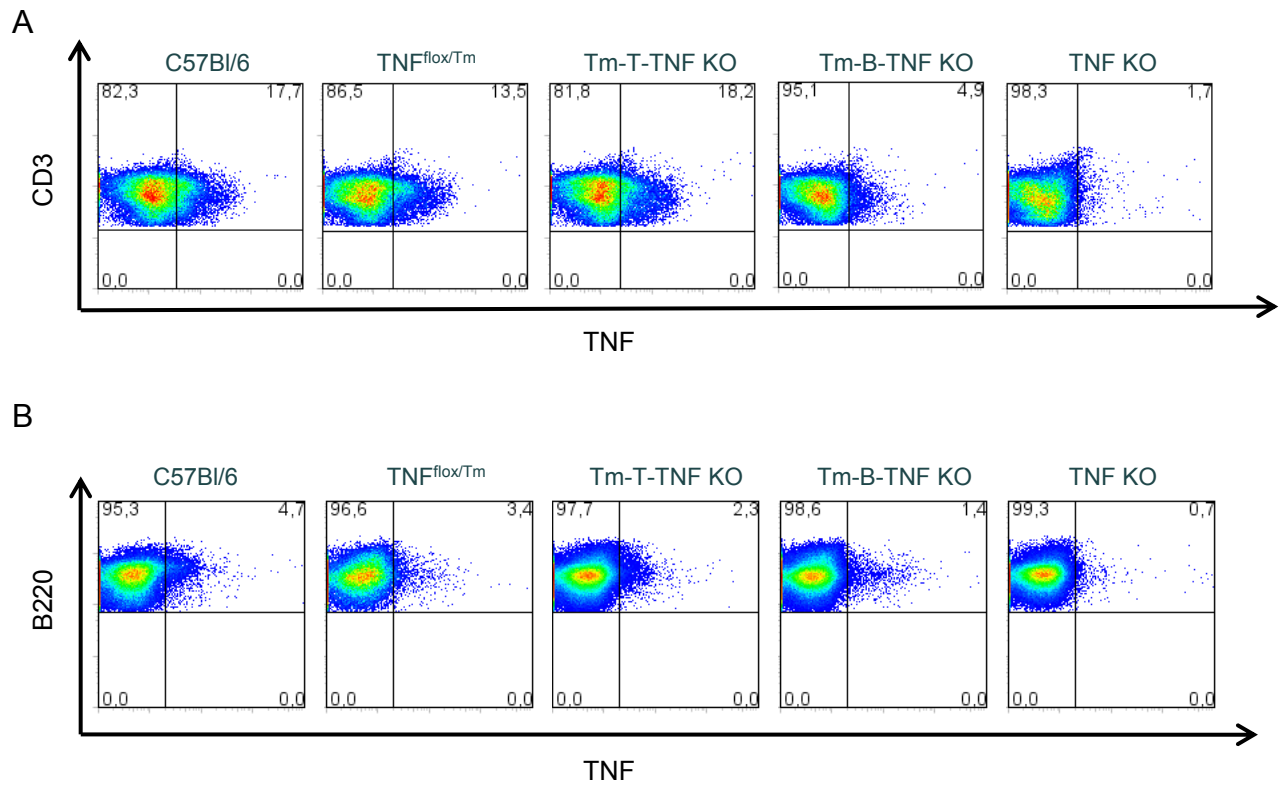


**Figure S10. TNF production by T and B cells in conditional TNF mutant mice.** T and B cells from Tm-T-TNF KO and Tm-B-TNF KO mice retain the capacity to produce TNF. Splenocytes from indicated mutant mice were stimulated with PMA/ionomycin in the presence of brefeldin A for 4h, and TNF expression by CD3<sup>+</sup> and B220<sup>+</sup> cells measured by flow cytometry. One of two experiments is shown. N=2 mice per group. Representative plots are shown.

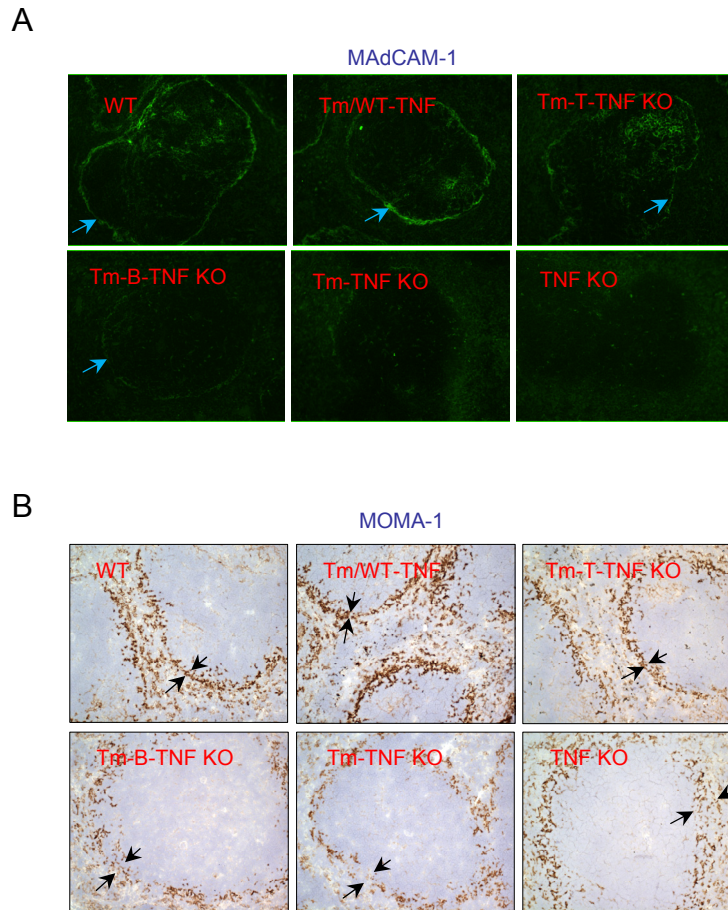


**Figure S11. Soluble TNF produced by B cells is essential for organization of the marginal zone.** **A.** Immunofluorescence staining of frozen spleen sections of indicated mutant mice with anti-MAdCAM-1 antibody. **B.** Immunostaining of frozen spleen sections with anti-MOMA-1 antibody. Note gradual reduction of MAdCAM-1 and MOMA expression in Tm-B-TNF KO, Tm-TNF KO and TNF KO mice (shown by arrows). Original magnification is x200. Representative images from one of two independent experiments (n=2 mice per group) are shown.

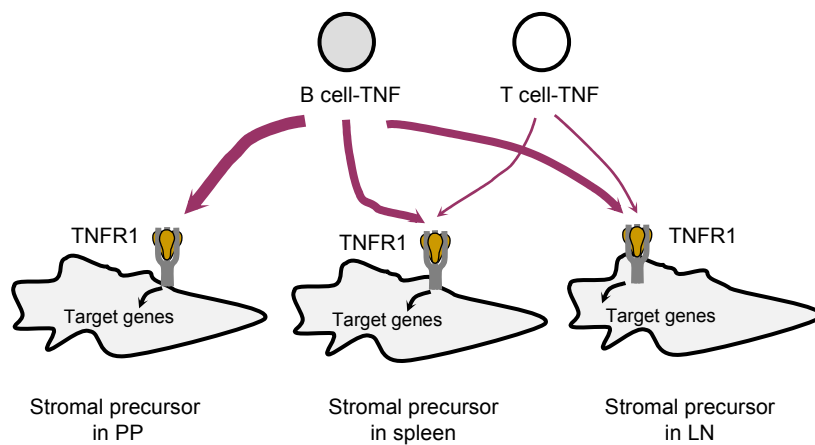


**Figure S12. Distinct requirements for cell-type specific TNF production in the organization of different secondary lymphoid tissues.** Generation of B cell follicles and FDC in spleen and mesenteric LN is predominantly regulated by soluble TNF from B cells (thick arrow), with a distinct contribution from TNF-expressing T cells (thin arrow). In contrast, PP structure is controlled predominantly by B cell-derived TNF (thick arrow). Stimulation of TNFR1 on stromal cell precursors triggers expression of TNF-dependent target genes required for generation of follicular dendritic cells and B cells follicles.

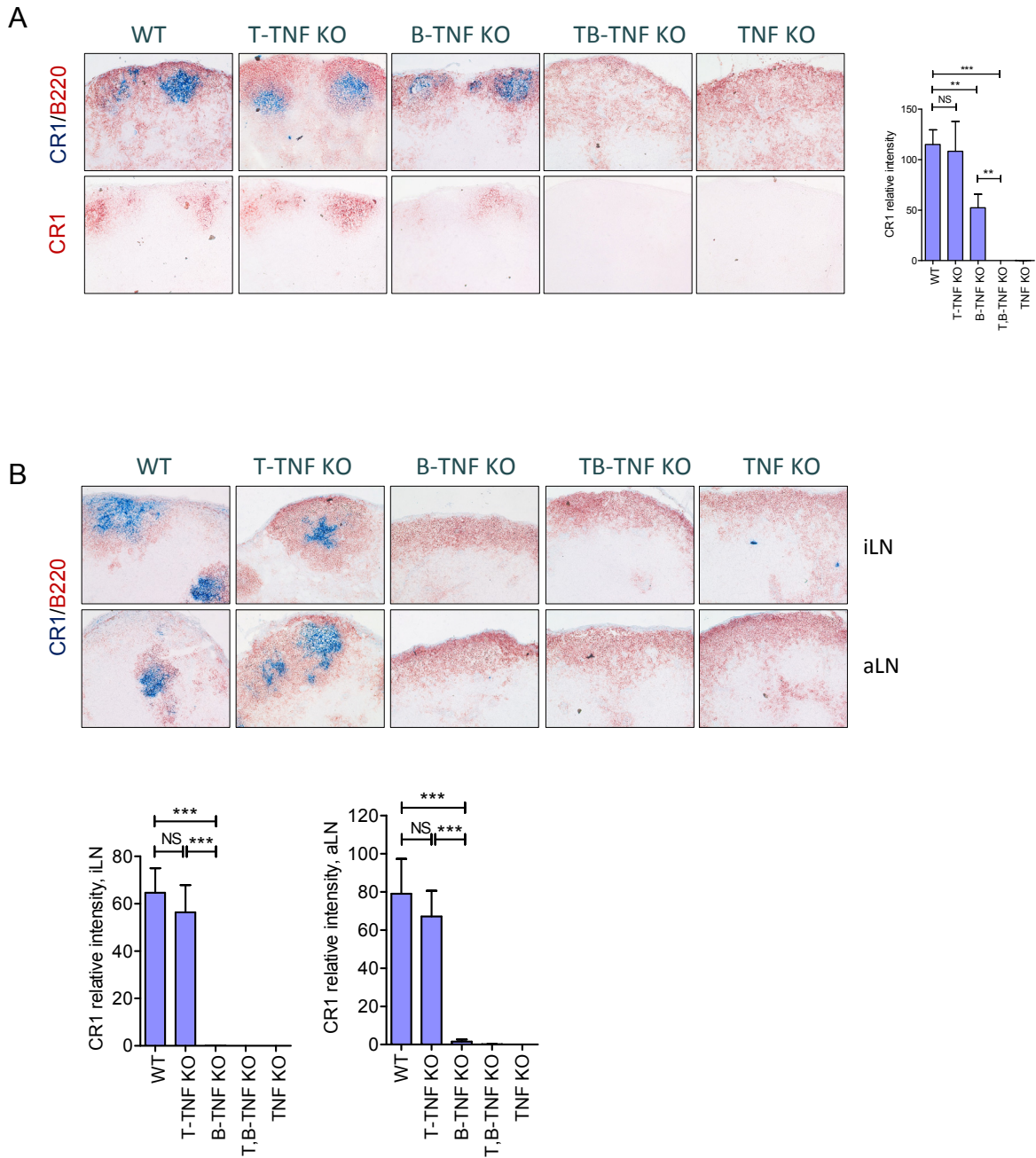


**Figure S13. Organization of naïve peripheral LNs is primarily dependent on TNF from B cells.** Mesenteric LN (**A**) and peripheral LN (**B**) from naïve conditional TNF deficient mice were stained with anti-B220 and anti-CR1 to visualize B cells follicles and FDC, respectively. Representative images from one of two independent experiments (n=3 mice per group) are shown. Original magnification is x200. Quantification of CR1 positive areas is presented as means  $\pm$  s.e.m. \*\* $P < 0.01$ , \*\*\* $P < 0.001$ .